X-551-70-322
PREPRINT

NASA TM X- 65330

TOTAL ELECTRON CONTENT MEASUREMENT WITH A GEOSTATIONARY SATELLITE DURING THE SOLAR ECLIPSE OF MARCH 7, 1970

S. RANGASWAMY
P. E. SCHMID

AUGUST 1970

GSFC

GODDARD SPACE FLIGHT CENTER
GREENBELT, MARYLAND

X-551-70-322
PREPRINT

TOTAL ELECTRON CONTENT MEASUREMENT WITH A GEOSTATIONARY SATELLITE DURING THE SOLAR ECLIPSE OF MARCH 7, 1970

S. Rangaswamy

National Academy of Science

P. E. Schmid

NASA/Goddard Space Flight Center

Presented at—

Upper Atmospheric Currents

and Electric Fields Symposium

Boulder, Colorado

August 17-21, 1970

TOTAL ELECTRON CONTENT MEASUREMENT WITH A GEOSTATIONARY SATELLITE DURING THE SOLAR ECLIPSE OF MARCH 7, 1970

S. Rangaswamy

National Academy of Science

P. E. Schmid

NASA/Goddard Space Flight Center

ABSTRACT

This note deals with the measurement of the total electron content of the ionosphere at the Goddard Space Flight Center, looking towards the geostationary satellite ATS-3 during the solar eclipse of March 7, 1970. Obscuration at this site was near total. Faraday rotation was measured using a stationary circularly polarized antenna and a dual channel phase lock receiver tuned to 137.350 MHz. By comparing the electrical phase of the two opposite circularly polarized components a continuous chart recording was made of Faraday rotation versus local time.

A depletion of about 25% in electron content was observed from first contact to the time of minimum electron content. The time variations of the electron content during the eclipse are briefly examined in the light of current theories of ionospheric processes.

CONTENTS

ILLUSTRATIONS

1. INTRODUCTION - THE MARCH 7, 1970, SOLAR ECLIPSE

The lunar shadow associated with the March 7, 1970, solar eclipse passed along the east coast of the United States between 1315 and 1400 hours EST. The shadow path is indicated in Figure 1. During the eclipse the NASA geostationary spacecraft Applications Technology Satellite-3 (ATS-3) was positioned at 275° East longitude, 0.53° South latitude, and 42,130 km altitude. Thus, the ATS-3 137.350 MHz transmission as recorded at the Goddard Space Flight Center (GSFC), Greenbelt, Maryland, traversed an ionosphere which during the eclipse experienced near total obscuration. The basic measurement made during the eclipse was relative spatial polarization of the linearly polarized ATS-3 transmissions as a function of time.

2. FARADAY ROTATION MEASUREMENT

As is well known, changes in the total electron content through the Earth's ionosphere can be related directly to Faraday rotation measurements. At GSFC Faraday rotation of the ATS-3 VHF signals were recorded during the eclipse by means of a two channel phase lock receiver, each channel having as an input one of the two circular components derived from the incoming linear polarization. Figure 2 presents the basic measurement technique where the linearly polarized signal is resolved into right and left hand circular components and then multiplied in an electronic phase detector whose full scale output is 2π radians where each π of rotation in spatial angle ϕ results in one cycle of electrical phase output. The receiver output, as shown in Figure 3, was recorded directly by an Esterline Angus chart recorder running at a rate of 1.5 inches per hour.

As shown in the records presented in Figure 3, during a normal day (such as February 25, 1970) ionization increases steadily during the morning hours up to the afternoon peak and then decays steadily as solar illumination decreases. Again with reference to Figure 3, a pronounced phase reversal occured during the eclipse as the lunar shadow intercepted the line-of-sight between the GSFC site and ATS-3 and ionization abruptly decreased. At approximately 1400 hours local time the integrated electron content again increased up to the usual diurnal reversal.

3. COMPUTATION OF TOTAL ELECTRON CONTENT

The Faraday rotation of the plane of polarization of a linearly polarized wave is given by the well known expression

$$\Omega = \frac{0.0297}{f^2} \int_{o}^{hs} N(h)\ M\ dh \qquad (1)$$

where M = H cos θ sec i

f = frequency of the wave

N(h) = electron density at a height h in the ionosphere

H = the geomagnetic field intensity in MKS units

θ = the angle between the ray and the geomagnetic field at the height h

i = the angle between the ray and the vertical at the height h

h_s = vertical height of the satellite

The quantity M was computed by knowing the geometry of the ray path connecting the receiver with the satellite and using the spherical harmonic expansion of Hendricks and Cain (1966) for the geomagnetic field. Figure 4 shows the variation of the quantity M with height along the ray path. It may be seen that M is a slowly varying function of height when compared with the possible variation of the electron density with height in the ionosphere. Hence, it is possible to approximate equation (1) by

$$\Omega = \frac{0.0297}{f^2} \overline{M} \int_{o}^{hs} N(h)\, dh \tag{2}$$

where $\overline{M}$ is the value of M at some ionospheric height chosen so as to make equations (1) and (2) numerically most equivalent. In the present calculations the value of $\overline{M}$ was chosen to be that of M at a height of 350 km along the ray path.

In earlier studies of ionospheric electron content during a solar eclipse signals from near-Earth satellites had to be used and this led to the variation of $\overline{M}$ over the duration of the eclipse due to the motion of the satellite and the consequent variation of the ray path. This is true of eclipse studies by the lunar radar technique too, though to a lesser extent. In the case of the March 7, 1970, eclipse, however, it was possible to make continuous measurements of Faraday rotation over a constant ray path by using the geostationary satellite ATS-3.

The accumulated Faraday rotation of the plane of polarization was plotted against time by using an arbitrary reference angle at some time t(0844 EST) and adding observed rotations relative to it from the original recording shown in Figure 3.

Figure 5 shows such a plot. For comparison the percentage obscuration of the solar disk as viewed from a point at a vertical height of 300 km on the ray path linking the GSFC receiving site with the ATS-3 is also shown in the Figure.

It is possible to compute changes in the total electron content (TEC) from the relative rotation plot by using equation (2). However, the computation of the absolute values of the TEC requires a knowledge of the absolute value of Faraday rotation of the plane of polarization. An attempt was made to resolve this ambiguity in the absolute angle of rotation by comparing it with ground based measurements. It is well known that the TEC is proportional to the maximum electron density of the ionospheric F2 layer and this fact has been used by Nakata (1966) to deduce the value of the absolute angle of Faraday rotation. Therefore, the relative angle of rotation was plotted against the square of the critical frequency of the F2 layer as measured at Wallops Island, Virginia. This was done because the maximum electron density, N_{max}, is proportional to the square of the critical frequency of the F2 layer. Figure 6 shows the resulting plot. It may be seen that the plot may be approximated by linear segments of differing gradients. The segment nearest to the vertical axis was fitted with a best fitting straight line, using the least squares criterion. This line is also shown in Figure 6.

The intercept of this straight line with the Y axis was taken to be the reference angle of rotation. The segment nearest to the vertical axis was chosen because it is numerically sound to assume a linear gradient only over a short range of values and the segment chosen needs the least amount of extrapolation to intercept the Y-axis.

Once the reference angle of rotation is known, it is easy to compute the absolute angles of rotation and hence to deduce the values of TEC using equation (2). The results of such a calibration are shown on the right hand side of Figure 5.

4. VARIATIONS OF THE TOTAL ELECTRON CONTENT (TEC) DURING THE ECLIPSE

The TEC variations show the normal diurnal increase around noon at the beginning of the eclipse. This increase continued for nearly 25 minutes after first contact. At 1245 EST the effect of the eclipse became apparent by a sharp decrease which continued until the minimum during the eclipse was reached at 1356 EST. The recovery of the TEC during the second phase of the eclipse was at first quite slow giving the impression of a flat minimum for about 30 minutes. From about 1425 EST the TEC started to increase rapidly until about 1510 EST when the post-diurnal-maximum trend took over and the TEC started to decrease again.

It may be observed from Figure 5 that the minimum in the TEC lags behind the time of maximum obscuration (1340 EST) by 16 minutes. The TEC decreased

from a value of about 6×10^{17} el/m^2 to about 4.4×10^{17} el/m^2 during the eclipse. Thus, the depletion in the columnar electron content during the eclipse was about 1.6×10^{17} el/m^2 or 25%.

5. DISCUSSION OF THE ECLIPSE EFFECTS

It is interesting to compare the variations of TEC with other ionospheric parameters like the electron content below the level of maximum ionization density (SHMAX) and the thickness parameter of the F2 layer (SCAT) as these yield more information about the layer structure. During the March 7, 1970, eclipse, intensive ground based sounding of the ionosphere was made at Wallops Island, Virginia, which was in the track of the eclipse. The analysis of these ionograms were done by the ESSA group to deduce parameters like the electron density at different heights N(h), SHMAX, SCAT, etc. Using the data furnished by ESSA, the time variations of SHMAX and SCAT were plotted and this is shown in Figure 7. It may be seen from the Figure that the bottom side electron content was reduced by nearly 40% during the eclipse. The value of SCAT which can be considered as the scale height at the height of the maximum electron density, HMAX, remained near 50 km for most of the time except near 1350 EST when there were rather large fluctuations between about 72 km to 36 km.

In fact, it may be seen from Figure 7 that the SHMAX and SCAT data show considerable oscillation and in the case of SCAT the oscillations make it difficult to see the trend of the main variations. An attempt was made to smooth the data by fitting least-squares polynomials to them. Figure 8 shows 7th degree polynomial fits to the SHMAX and SCAT data along with the TEC variations. It may

be observed from the Figure that the bottom side electron content more or less follows the total electron content. However, its response to the eclipse is faster in both phases of the eclipse. The smoothed variation of the SHMAX data shows a delay of about 8 minutes between the minimum and the time of maximum obscuration. The smoothed SCAT data show two minima with a maximum around the time of the minimum in TEC.

The ratio of the TEC to SHMAX is another parameter defining the layer structure. This quantity which we shall call RATIO is plotted in Figure 9 along with SCAT and HMAX, the height of the maximum electron density of the F2 layer. It may be seen that the value of RATIO during the eclipse fluctuates between 2.8 to 3.6. The value of RATIO for the classical Chapman layer is 3.15. It is interesting to see that while the SCAT variations are roughly in phase with those of HMAX, the RATIO variations are roughly anti-phase to those of SCAT. This is what one would normally expect in view of the fact that HMAX divides the top side from the bottom side and an increase of HMAX will normally decrease RATIO. This is particularly true in view of the fact that SCAT is related to the electron and ion temperatures (Stubbe, 1970) and will normally increase with increase of HMAX. An increase of SCAT will further increase SHMAX. However, the effects of downward diffusion of ionization coupled with the cooling of the plasma during the eclipse may lead to departures from this simple pattern.

During the first phase of the eclipse RATIO is seen to increase up to about 1320 EST. This is probably due to the fact that the bottom side ionosphere is

responding more rapidly than the top side to the eclipse. The eventual reduction of the top side ionization coupled with the downward diffusion of ionization (Stubbe, 1970) reduces RATIO later on. After the time of maximum obscuration the bottom side ionosphere recovers more rapidly than the top side which makes RATIO decrease still further. Finally the response of the top side ionosphere to the second phase of the eclipse coupled with the decrease in downward diffusion of ionization (Stubbe, 1970) leads to the increase of RATIO again.

Stubbe (1970) has made a recent theoretical study of the time variations of the ionosphere over Wallops Island during the eclipse of March 7, 1970. He did this by the numerical solution of ten coupled differential equations, including the continuity equations for different ions, the heat conduction equations and the equations of motion describing neutral winds. The time dependent solutions yield such quantities as electron and ion concentrations and temperatures and hence layer parameters such as integrated electron content and semithickness of the layer. Stubbe predicted the following for the March 7, 1970, eclipse:

1. The ratio of the TEC to the bottom side electron content will have a sharp maximum of 3.3 at the time of the maximum obscuration as compared to the value 2.6 for the reference atmosphere.
2. The TEC will have a minimum at the time of maximum obscuration which is about a factor of two smaller than the corresponding value in the normal ionosphere.

From our study we note that RATIO increased from a value of about 2.9 at 1200 EST to a maximum of 3.6 at 1320 EST. These values are in good agreement with Stubbe's predictions. The TEC has a minimum during the eclipse which is smaller by a factor of 1.5 than the corresponding value in the normal ionosphere. However, as pointed out earlier, this minimum in TEC is not coincident with the time of maximum obscuration but lags behind it by 16 minutes.

ACKNOWLEDGEMENT

We are grateful to Mr. C. R. Newman of the Goddard Space Flight Center for his help in the computation of the optical obscuration function during the eclipse.

REFERENCES

1. Hendricks and Cain, 1966, J. Geophys. Res. 71, 346-47.
2. Nakàta, 1966, Radio Science, 1, 1145-48.
3. Stubbe, 1970, J. Atmosph. Terr. Phys., 32, 1109-16.

FIGURE CAPTIONS

Figure 1. Solar Eclipse

Figure 2. Polarization Measurement Scheme

Figure 3. Faraday Rotation from ATS-3

Figure 4. M-Factor Variation with Height along Ray Path Linking GSFC with ATS-3

Figure 5. Total Electron Content and Optical Obscuration Function During the Solar Eclipse of March 7, 1970

Figure 6. Relative Faraday Rotation Angle Versus $(f_0 f_2)^2$

Figure 7. Variation of SHMAX and SCAT During Eclipse (Raw Data)

Figure 8. Smoothed Variation of SHMAX and SCAT along with TEC and Obscuration Function

Figure 9. Variation of SCAT, RATIO, and HMAX During the Eclipse

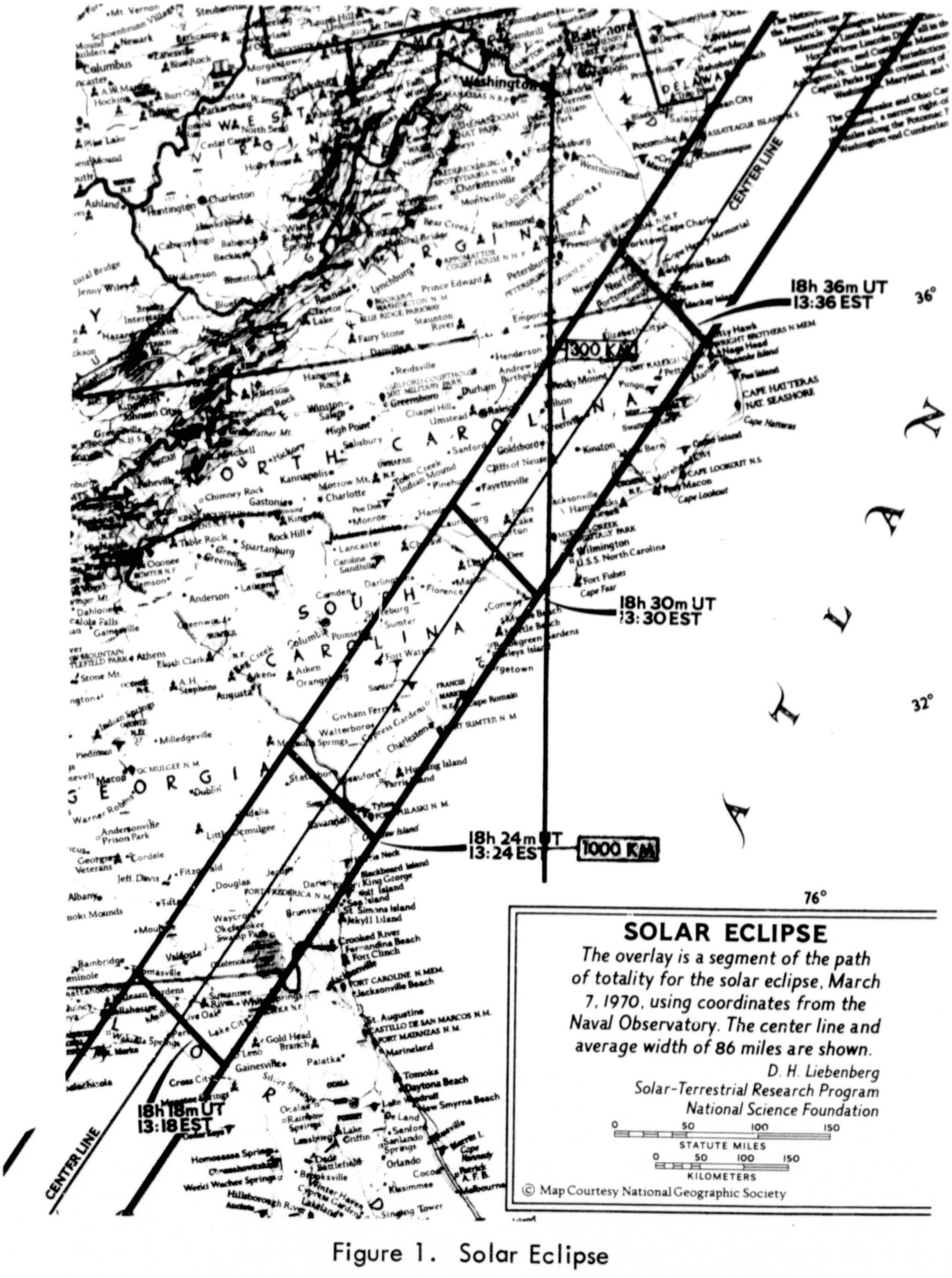

Figure 1. Solar Eclipse

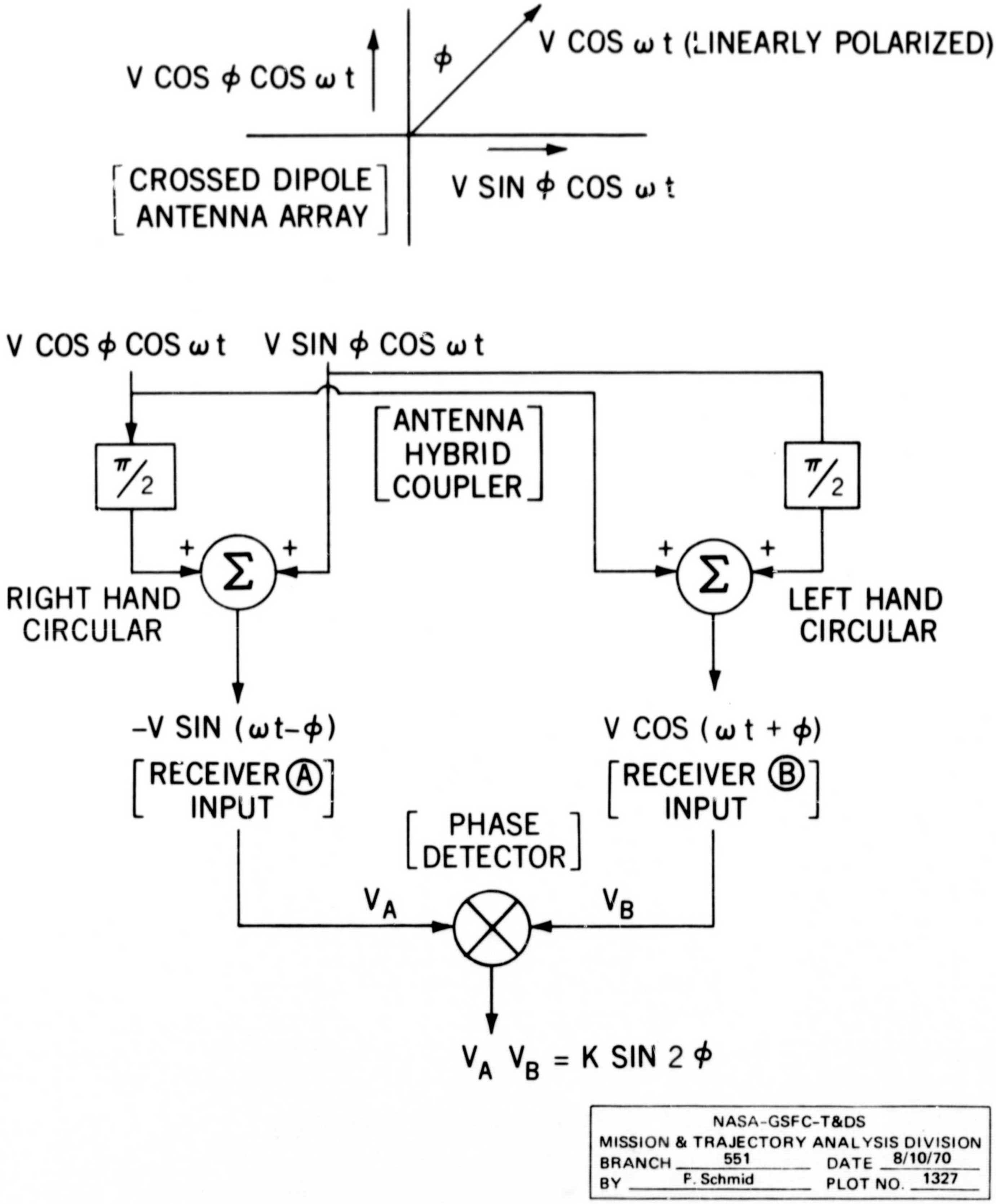

Figure 2. Polarization Measurement Scheme

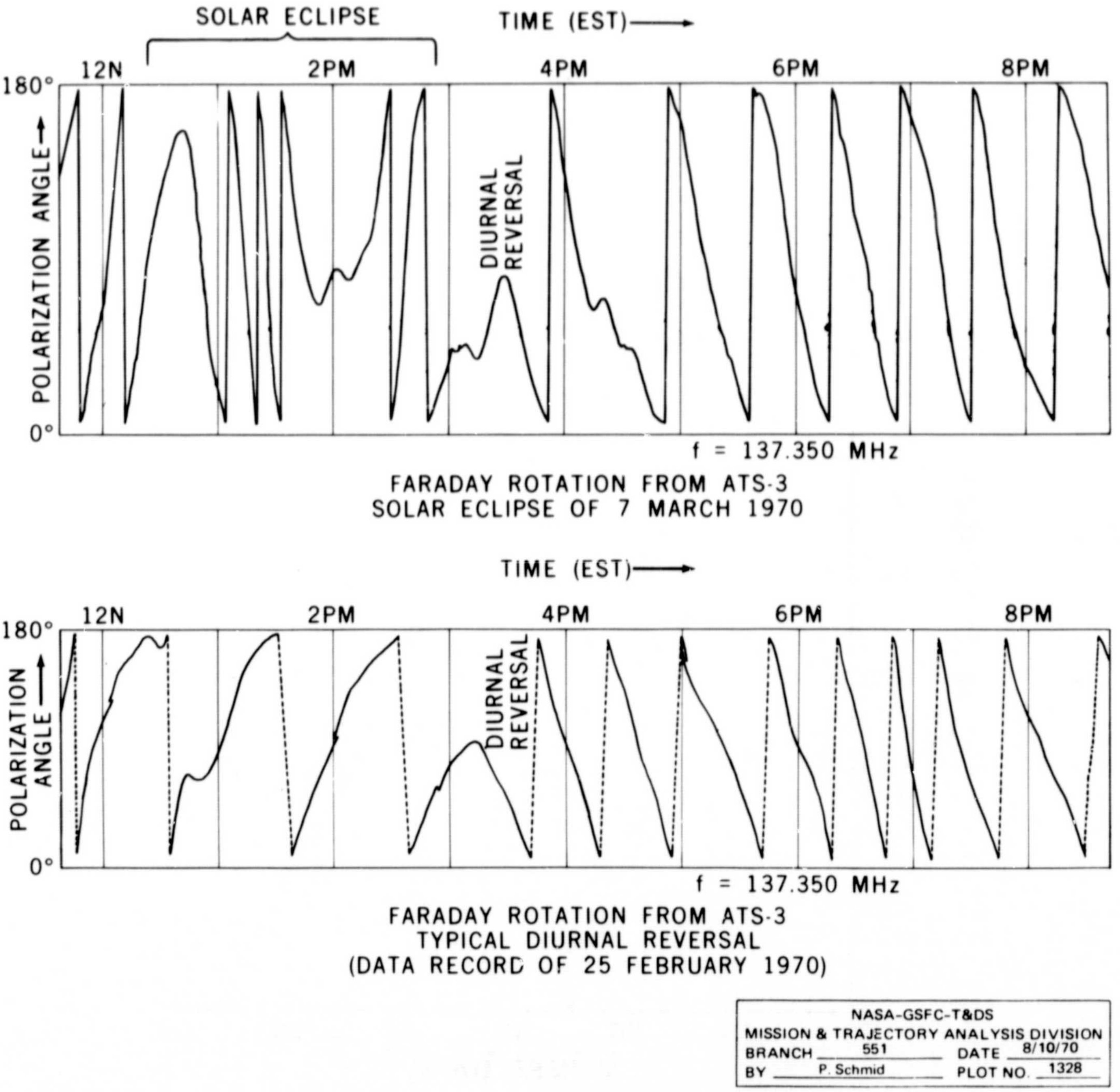

Figure 3. Faraday Rotation from ATS-3

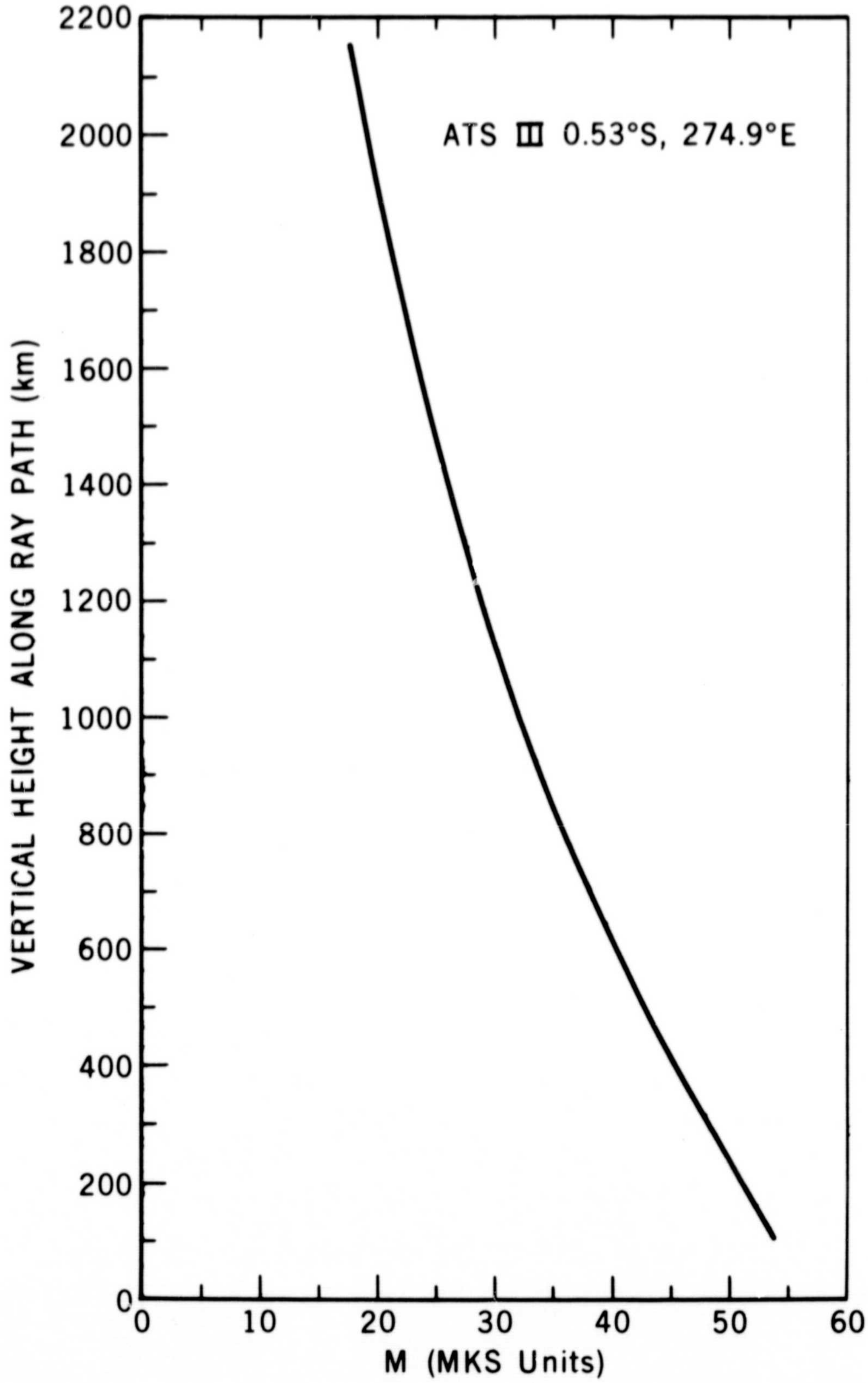

NASA-GSFC-T&DS
MISSION & TRAJECTORY ANALYSIS DIVISION
BRANCH 551 DATE 8/10/70
BY S. Rangaswamy PLOT NO. 1329

Figure 4. M-Factor Variation with Height along Ray Path Linking GSFC with ATS-3

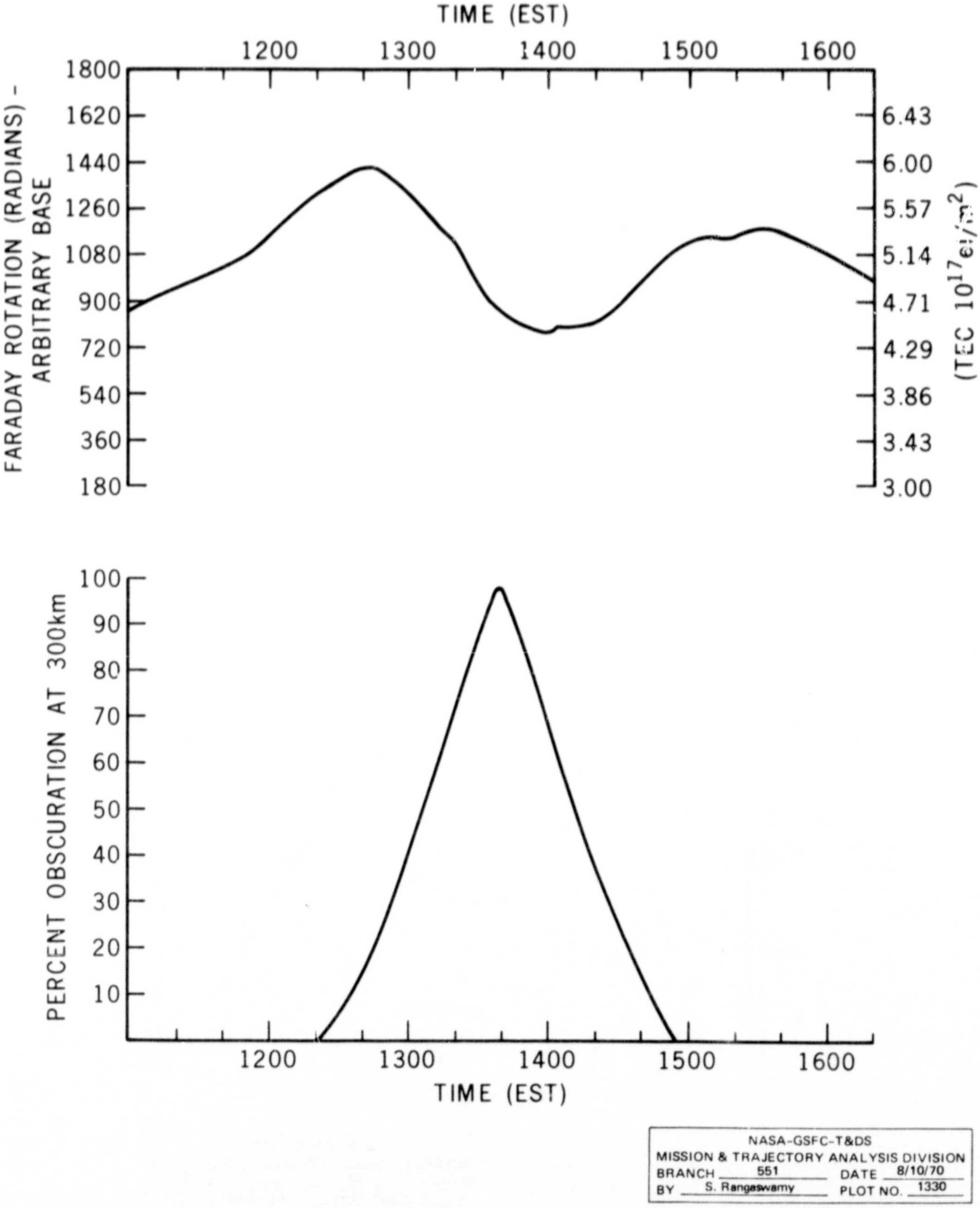

Figure 5. Total Electron Content and Optical Obscuration Function During the Solar Eclipse of March 7, 1970

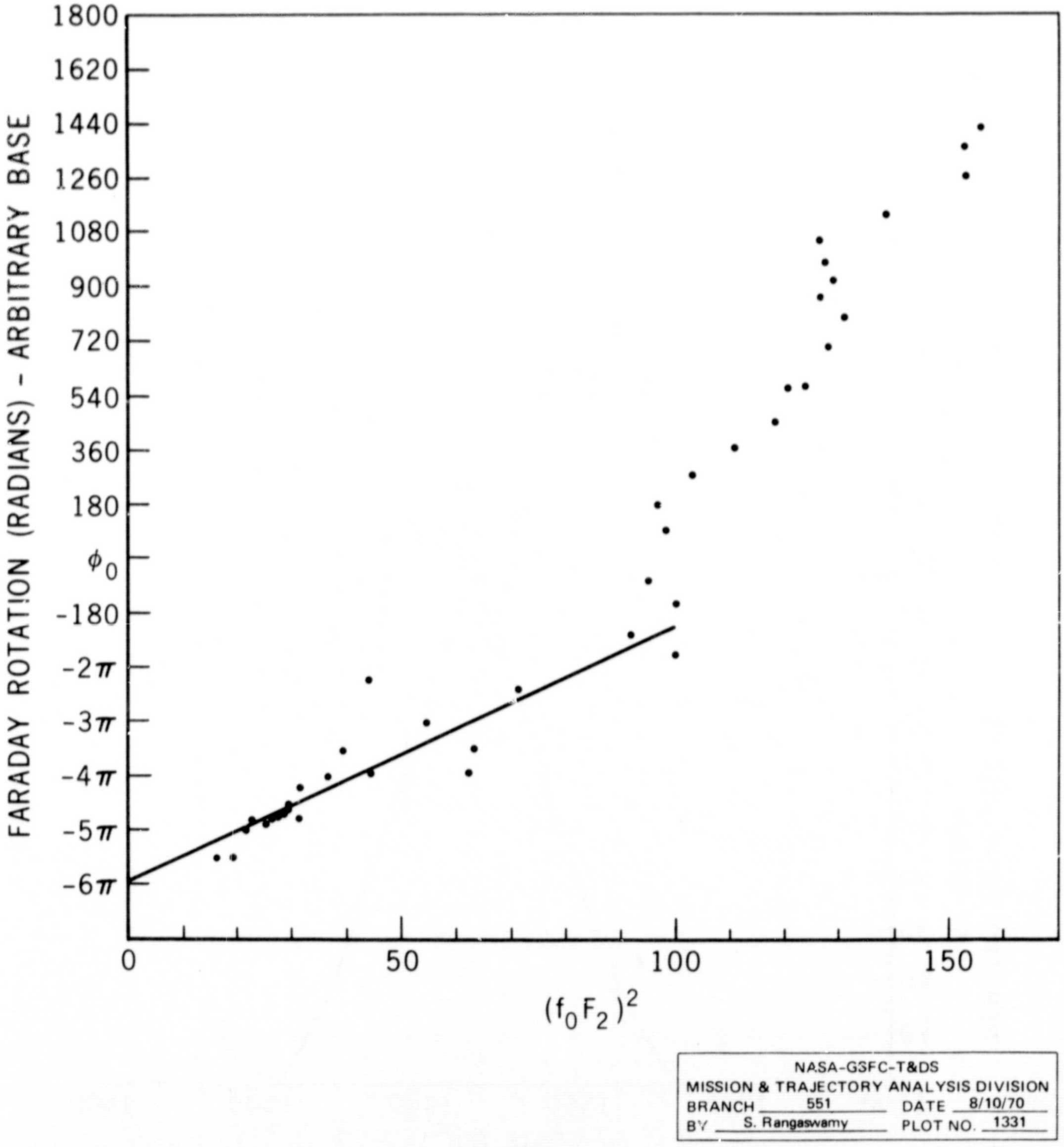

Figure 6. Relative Faraday Rotation Angle Versus $(f_0f_2)^2$

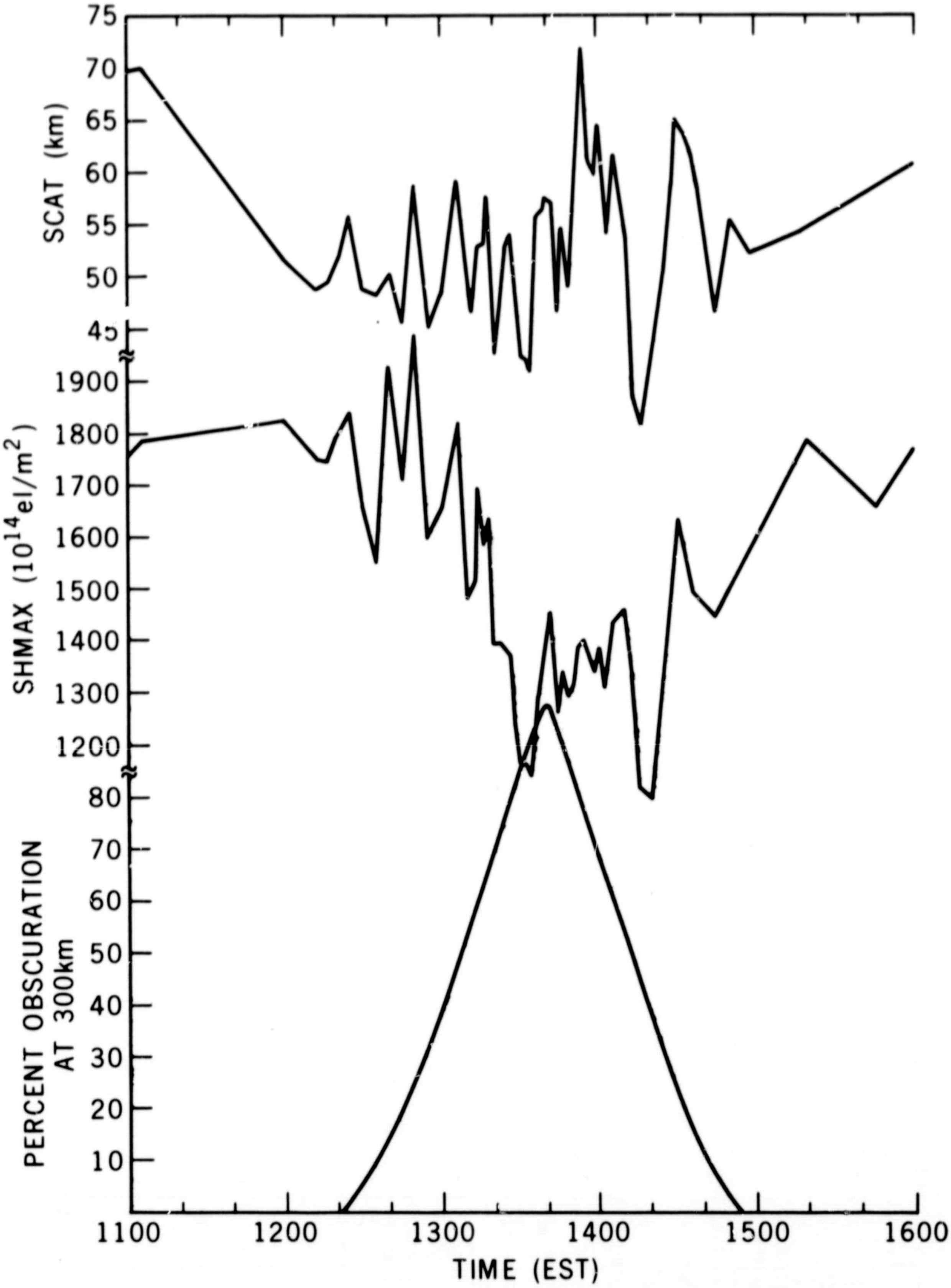

NASA-GSFC-T&DS	
MISSION & TRAJECTORY ANALYSIS DIVISION	
BRANCH 551	DATE 8/10/70
BY S. Rangaswamy	PLOT NO. 1334

Figure 7. Variation of SHMAX and SCAT During Eclipse (Raw Data)

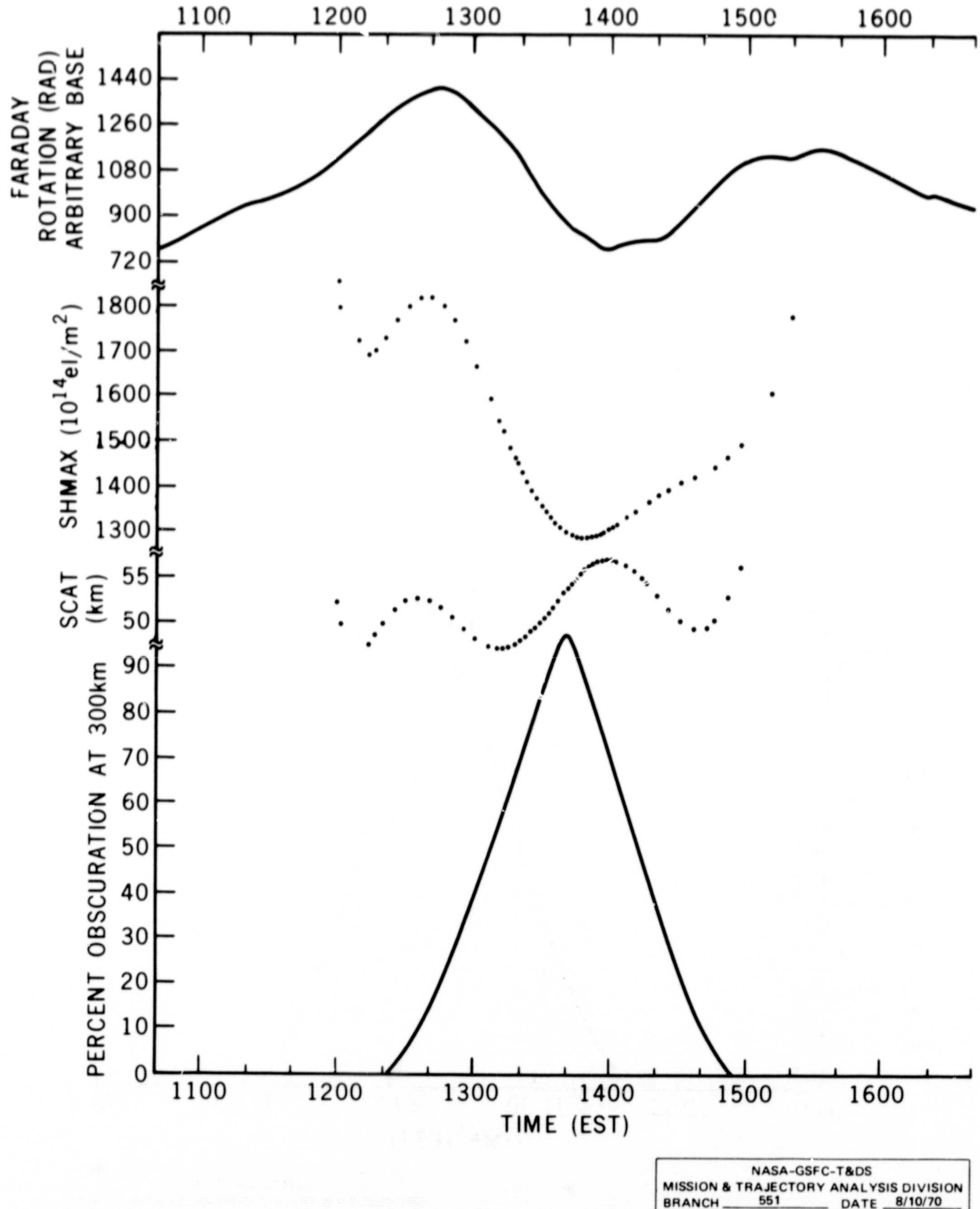

Figure 8. Smoothed Variation of SHMAX and SCAT along with TEC and Obscuration Function

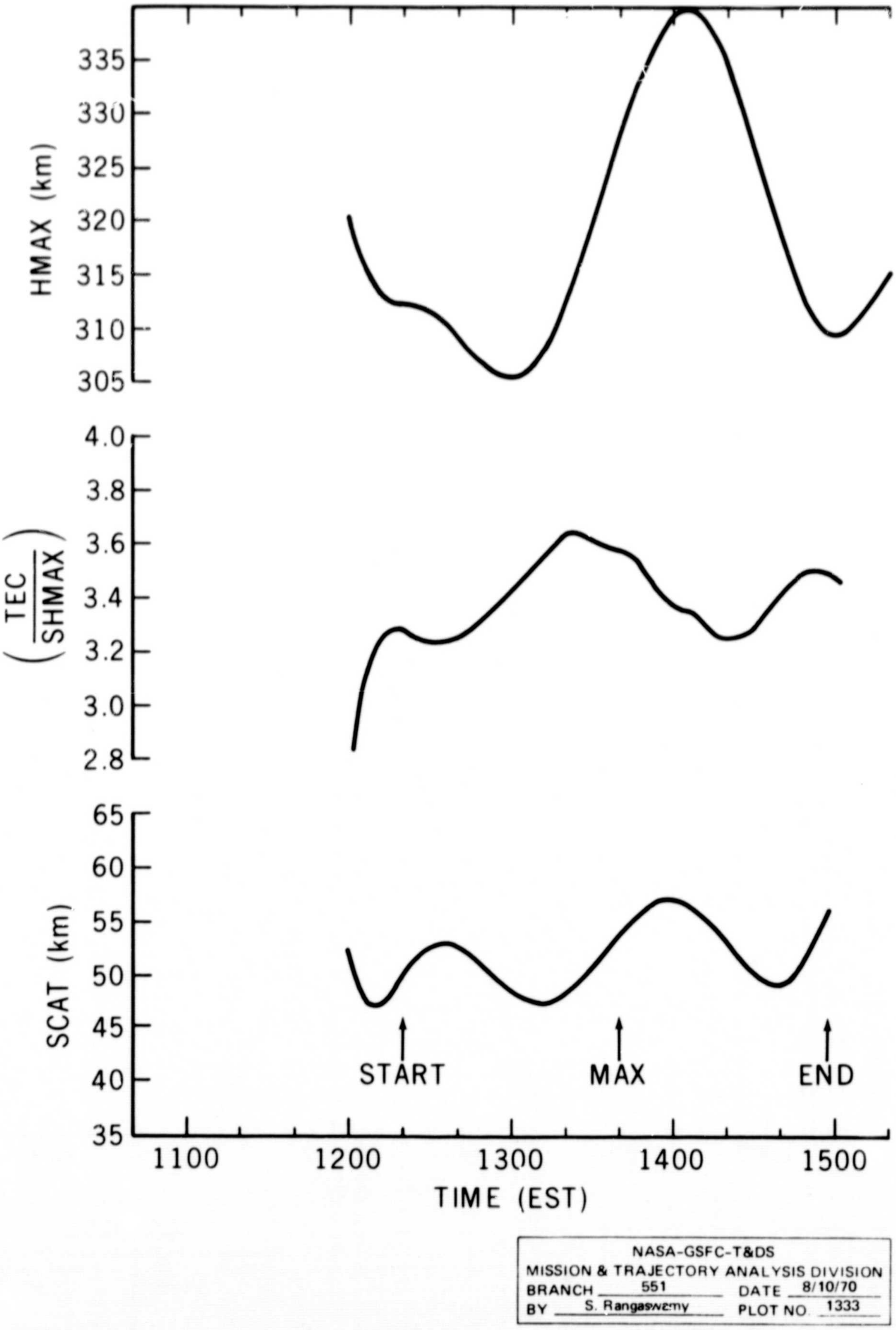

Figure 9. Variation of SCAT, RATIO, and HMAX during the Eclipse